Combustion and Flame 224 (2021) 126–135

Contents lists available at ScienceDirect

Combustion and Flame

journal homepage: www.elsevier.com/locate/combustflame

A physics-based approach to modeling real-fuel combustion chemistry – VII. Relationship between speciation measurement and reaction model accuracy

Rui Xu*, Hai Wang

Department of Mechanical Engineering, Stanford University, Stanford, CA 94305-3032, USA

ARTICLE INFO

Article history:
Received 9 July 2020
Revised 9 October 2020
Accepted 10 October 2020
Available online 28 October 2020

Keywords:
HyChem
Jet fuel
Kinetic modeling
Uncertainty analysis

ABSTRACT

The HyChem (hybrid chemistry) approach has been proposed recently for modeling high-temperature combustion of real, multicomponent fuels. The approach combines lumped reaction steps for fuel thermal and oxidative pyrolysis with detailed chemistry for oxidation of the resulting pyrolysis products. The 14 independent model parameters in the lumped reaction steps are determined by matching the time histories of key pyrolysis products of the fuel, obtained notably from the Stanford shock tube and laser diagnostics facilities, and from flow reactor experiments. The prediction accuracy of HyChem model depends on the availability of the speciation data and their accuracy. In the present work, we carry out comprehensive Monte Carlo analysis of model predictions with respect to species measurement using the Jet A HyChem model as the test case. We assess the impact of the measured fuel pyrolysis products, including ethylene (C_2H_4), methane (CH_4), propene (C_3H_6), *iso*-butene (*i*-C_4H_8), 1-butene (1-C_4H_8), benzene (C_6H_6), and toluene (C_7H_8) on HyChem predictions using ignition delay time and laminar flame speed as test cases. The results show that the speciation data are necessary to obtain reliable predictions for the laminar flame speed and ignition delay time at and above 1200 K. Additional measurement targets (e.g., CO and CH_2O) are proposed for future HyChem model development, especially in improving model predictions for ignition delay time.

1. Introduction

Proposed recently, the HyChem (hybrid chemistry) approach [1–4] offers an alternative path to modeling high-temperature combustion chemistry of real, liquid fuels. The approach has been applied to a range of practical fuels, including jet fuels [2–4], rocket fuels [2], and gasoline fuels [5], some of which are multicomponent and derived from a petroleum origin, while others are single-component and of a renewable origin. Blends of a single-component, bio-derived jet fuel with a conventional jet fuel have also been studied within the HyChem framework [3]. Because of its compact size and with further model reduction, the HyChem models are found to be particularly useful in simulating turbulent combustion of real fuels [6,7] and computational fluid dynamics under realistic combustor conditions (see, e.g. [8,9]). A HyChem model has been combined with a recent NO_x model [10] to simulate NO_x production in a series of premixed stagnation flames of a conventional Jet A with satisfactory results [11].

HyChem exploits several key factors in large-hydrocarbon combustion: a) fuel pyrolysis occurs in the flame front or in the induction period leading to ignition at high temperatures and is usually much faster than the oxidation of the resulting pyrolysis products; b) there are only a few key fuel pyrolysis products that need to be followed as opposed to the fuel itself which usually contains substantially more components. The disparity in time scales of fuel pyrolysis and the oxidation of the pyrolysis products at high temperatures [1,12] enables us to express the overall kinetic process of the fuel oxidation in two sequential, loosely coupled processes/submodels: i) an experimentally constrained, lumped fuel thermal and oxidative pyrolysis submodel and ii) a detailed foundational fuel chemistry model that describes oxidation of the resulting pyrolysis products. Suffice it to note that many of the concepts involved in the HyChem approach are not new. For example, lumped reaction modeling has been discussed in simulating complex hydrocarbon combustion a long time ago (see, for example, [13]). Williams and coworkers have advocated a

* Corresponding author.
E-mail address: ruixu@stanford.edu (R. Xu).

https://doi.org/10.1016/j.combustflame.2020.10.023
0010-2180/

"simplified" reaction modeling approach and used it in modeling JP-10 combustion [14,15].

In practice, HyChem models are developed and tested in two separate steps. In the first step, the thermal/oxidative pyrolysis submodel of the fuel is formulated first on the basis of elemental conservation. Coupled with the foundational fuel chemistry model, the kinetic parameters of the pyrolysis model are determined by species time history measurements in shock tube and flow reactor through an inverse value problem. For common jet fuels, the key intermediates of the pyrolysis process [1,2] are typically ethylene (C_2H_4), methane (CH_4), propene (C_3H_6), *iso*-butene (i-C_4H_8), 1-butene (1-C_4H_8), benzene (C_6H_6) and toluene (C_7H_8). In the second step, the model is tested against global combustion properties, including ignition delay time, laminar flame speed, and laminar non-premixed flame extinction strain rate.

The HyChem approach bypasses some of the difficulties encountered in the commonly adopted surrogate fuel approach (e.g., [16,17]). In essence, the HyChem approach seeks to unravel the complex chemistry of real fuel combustion by establishing the kinetic relationship between fuel combustion properties and independent variables directly related to these properties. It has been argued [1,2] that these independent variables are the composition of the fuel pyrolysis products, rather than the detailed molecular functionalities in the original fuel molecules. Since the key fuel pyrolysis products are rather few and their productions are fast [1], the HyChem approach does not make an attempt to follow the detailed chemical process of fuel breakdown. Rather, it utilizes the measured pyrolysis products as the input to the model. At the fundamental level, the key difference between the HyChem and surrogate approaches is nothing more than where we start to carry out the lumping procedure: the surrogate seeks lumping at the fuel composition level, while HyChem seeks lumping beyond fuel pyrolysis.

The HyChem approach has its own drawbacks. Like the surrogate approach, the accuracy of the HyChem fuel pyrolysis submodel is subject to the accuracy of model assumptions, and as importantly, to the availability and completeness of the speciation data and their measurement uncertainties. While the model assumptions have been discussed and justified extensively in earlier studies [1,2], several questions remain; and this will be the focus of the present work. In particular, given the amount of data available and used, it is possible that the model parameter set is not unique or the model is not mathematically closed. As the result, there is a feasible parameter set within which all combinations of the parameter values can reproduce the speciation data, yet within this feasible parameter set the model diverges in combustion property prediction. Two related questions are: i) are the speciation data we used sufficient in scope and accuracy in making accurate and converged predictions of global combustion properties, and ii) what additional speciation data might be needed to make improvements? To answer these questions, we take the Jet A fuel (designated as POSF10325 in the National Jet Fuel Combustion Program [18]) and its associated HyChem reaction model [2] as our test case. We carry out Monte Carlo (MC) analysis to determine the feasible parameter set within which the HyChem model reproduces the time profiles of the key pyrolysis species. The feasible set is examined for convergence of the respective HyChem parameters and tested for predicting the global combustion properties of ignition delay and laminar flame speed. We then carry out similar analyses by relaxing some or all available speciation constraints to address two additional questions: i) what is the role of speciation data in HyChem model development, and ii) what are the minimum set of data needed for obtaining a reasonably reliable HyChem model.

2. HyChem model assumptions and approach

We briefly review the HyChem assumptions and formation here. Details can be found in [2]. Some key HyChem assumptions are:

(1) High-temperature combustion of large hydrocarbon fuels follows a decoupled reaction process: fuel pyrolysis first, oxidation of the pyrolysis products second.
(2) The pyrolysis process is not rate limiting and can be described by lumped reaction steps, yielding several key pyrolysis products as the intermediates with fairly well defined, detailed combustion chemistry.
(3) For conventional distillate fuels, the number of key pyrolysis products is small. They are: C_2H_4, CH_4, C_3H_6, i-C_4H_8, 1-C_4H_8, C_6H_6, and C_7H_8.
(4) The oxidation of the pyrolysis products is rate limiting and must be treated by detailed chemistry.

The approach expresses the fuel pyrolysis and oxidation of the pyrolysis products in two submodels. Fuel pyrolysis is modeled by experimentally constrained lumped reaction steps. The oxidation of the pyrolysis products is described by a detailed foundational fuel chemistry model; USC Mech II [19] is used here for that purpose. The lumped reactions are cast into the following reactions:

$$\begin{aligned} C_mH_n \rightarrow\ & e_d(C_2H_4 + \lambda_3C_3H_6 + \lambda_{4,i}i\text{-}C_4H_8 + \lambda_{4,1}1\text{-}C_4H_8) \\ & + b_d[\chi C_6H_6 + (1-\chi)C_7H_8] + \alpha H + (2-\alpha)CH_3 \end{aligned} \quad \text{(R1)}$$

$$\begin{aligned} C_mH_n + R \rightarrow\ & RH + \gamma CH_4 + e_a(C_2H_4 + \lambda_3C_3H_6 \\ & + \lambda_{4,i}i\text{-}C_4H_8 + \lambda_{4,1}1\text{-}C_4H_8) \\ & + b_a[\chi C_6H_6 + (1-\chi)C_7H_8] + \beta H + (1-\beta)CH_3 \end{aligned} \quad \text{(R2-R7)}$$

where R = H, CH_3, OH, O_2, HO_2, and O. For real fuels, m and n are usually non-integer values. In the current HyChem formulation, however, we approximate m and n as integers, since most computer codes can only handle integer molecular formula [2]. Reaction (R1) is the C–C fission reaction of the fuel "molecule", eventually producing H and CH_3 radicals. Reactions (R2-R7) describes the H-abstraction of the fuel "molecule" followed by β-scission of the resulting fuel radical. Since the H-abstraction reaction producing the fuel radical is rate limiting while the following β-scission is facile, the two reaction processes are combined into a single step, as described by Reactions (R2-R7). Furthermore, the stoichiometric parameters of the pyrolysis products in Reactions (R2-R7) are assumed to be independent of the H-abstraction reacting radicals/molecules. The detailed explanations are presented in an earlier study using n-hexane thermal decomposition as an example [1]. Briefly, for H-abstraction of a large hydrocarbon molecule C_mH_n, the equilibrium concentration of the resulting radical isomers (C_mH_{n-1}) is primarily determined by their Gibbs free energies. The composition of the radical isomers directly determines the composition of the pyrolysis product, regardless of what the H-abstraction reacting radicals/molecules are.

With carbon and hydrogen elemental conservations, the stoichiometric coefficients, e_d, e_a, b_d, and b_a can be treated as dependent variables,

$$e_d = \frac{[-(4-\chi)m + (7-\chi)n/2 + 3\alpha + \chi - 13]}{3(2 + 3\lambda_3 + 4\lambda_{4,i} + 4\lambda_{4,1})} \quad (1)$$

$$e_a = \frac{[-(4-\chi)m + (7-\chi)n/2 + 3\beta - (10-\chi)\gamma - (10-\chi)]}{3(2 + 3\lambda_3 + 4\lambda_{4,i} + 4\lambda_{4,1})} \quad (2)$$

$$b_d = (m - n/2 + 1)/3 \quad (3)$$

Table 1
Summary of independent stoichiometric parameters of the HyChem Jet A model and test cases considered in the current work.

Parameter	Description	Method of determination[a]	Range	Nominal value[c]	MC cases and parameter ranges[e]			
					1	2	3	4
α	Number of H atoms from (R1) per C_mH_n	ST	[0, 2]	0.50	d	d	[0, 2]	[0, 2]
β	Number of H atoms from (R2-R7) per C_mH_n	ST	[0, 1]	0.30	d	d	[0, 1]	[0, 1]
γ	CH_4 yield in addition to H-abstraction by CH_3 in (R2-R7)	ST	[0, γ_{max}][b]	0.45	d	[0, 0.9]	[0, 0.9]	[0, γ_{max}]
λ_3	C_3H_6-to-C_2H_4 yield	FR, ST	[0, ∞]	0.47	[0.43, 0.51]	[0, 0.94]	[0, 0.94]	[0, 2]
$\lambda_{4,i}$	i-C_4H_8-to-C_2H_4 yield	FR, ST	[0, ∞]	0.05	[0.04, 0.06]	[0, 0.1]	[0, 0.1]	[0, 2]
$\lambda_{4,i}$	1-C_4H_8-to-C_2H_4 yield	FR, ST	[0, ∞]	0.15	[0.13, 0.17]	[0, 0.3]	[0, 0.3]	[0, 2]
χ	C_6H_6-to-(C_6H_6 + C_7H_8) yield	FR, ST	[0, 1]	0.51	[0.47, 0.55]	[0, 1]	[0, 1]	[0, 1]

[a] ST: shock tube species time histories of C_2H_4 and CH_4; FR: flow reactor. [b] γ_{max} is derived from Eqn. (2) by setting $e_a \geq 0$: $\gamma_{max} = -1 + [-(4-\chi)m + (7-\chi)n/2 + 3\beta]/(10-\chi)$. [c]Values used in the nominal Jet A model [1]. [d] The parameter values are determined from C_2H_4 and CH_4 time history data (and their uncertainties). In the MC procedure, the initial ranges of α, β, and γ are chosen to be those of Case 3. The randomly sampled reaction models are then down-selected to a feasible set with all models in the set give C_2H_4 and/or CH_4 time history profiles that lie inside the experimental uncertainty band. See text. [e] The MC sampling uses uniform distributions over the respective parameter ranges stated.

$$b_a = (m - n/2 + \gamma + 1)/3 \tag{4}$$

while α, β, γ, λ_3, $\lambda_{4,i}$, $\lambda_{4,1}$, and χ are the independent stoichiometric parameters. The above formulation contains a total of 14 undetermined parameters in all; seven of them are the stoichiometric parameters and the other seven are the rate coefficients k_i (i = 1, 2, ..., 7).

In Table 1, the physical ranges of the stoichiometric parameters are provided, and these bounds are defined by elemental conservation. The parameters λ_3, $\lambda_{4,i}$, and $\lambda_{4,1}$ are the C_3H_6-to-C_2H_4, i-C_4H_8-to-C_2H_4, and 1-C_4H_8-to-C_2H_4 yield ratios, respectively; χ is the ratio of C_6H_6 to the sum of C_6H_6 and C_7H_8 yields. These ratio values are usually estimated first from oxidative pyrolysis experiments in a flow reactor [2]. The parameters α and β represent the number of H radicals generated from C–C fission reaction (R1) and from H-abstraction reaction (R2-R7) followed by β-scission, respectively. γ is the CH_4 yield per fuel "molecule" in addition to H-abstraction from the CH_3 radical. The seven rate coefficients k_i (i = 1, 2, ..., 7) are estimated initially from the analogous reactions (e.g., of n-dodecane in JetSurF 2.0 [20]). Briefly, k_1 is assumed to be the sum of all the n-dodecane C–C bond fission reaction rates. The rate coefficient k_2 is initially estimated to be the sum of the H-abstraction rates of n-dodecane by H atom, producing n-dodecyl radicals. Similarly, k_3-k_7 are the sum of rates of n-dodecane H-abstraction by CH_3, OH, O_2, HO_2, and O, respectively. Then, these rate coefficients, together with α, β, and γ, and the ratio parameters discussed earlier are jointly determined by matching the C_2H_4 and CH_4 time history data from shock-tube thermal and oxidative pyrolysis experiments of the fuel in an inverse problem. The values of the ratio parameters are adjusted accordingly during this process, and their final values are always close to those directly measured in the flow reactor [1,2]. For Jet A, the nominal values of the stoichiometric parameters are listed in Table 1 for reference. The rate coefficients can be found in the original publication [1]. Suffice it to note that the HyChem model predictions of global combustion properties are more sensitive to stoichiometric parameters (e.g., β and λ_3); and less to the rate coefficients.

3. Simulation method and cases

Kinetic modeling is carried out using the Sandia Chemkin package [21]. Fuel pyrolysis is simulated isobarically and adiabatically. The ignition delay time (τ_{ign}) is computed as the time to the maximum rate of OH* production under the isochoric and adiabatic condition. The laminar flame speed (S_u°) is calculated using PREMIX [22]with multicomponent transport and thermal diffusion.

The Monte Carlo (MC) cases, listed in Table 1, are designed to address the questions raised in the Introduction section. Case 1 is the base case built on the actual experimental speciation values and their respective uncertainties. The ratio parameter (λ's and χ) values are sampled within their respective uncertainties in the Stanford flow reactor, which are discussed in [2]. The α, β, and γ values are sampled implicitly from C_2H_4 and CH_4 time histories measured in the Stanford shock tube facilities and their respective uncertainties by a MC shooting method, as will be discussed later. This case features the feasible parameter set of the HyChem model for the Jet A fuel.

Case 2 essentially uses C_2H_4 speciation as the only constraint and tests the question about how accurate the HyChem model can be when it is constrained by this dominant pyrolytic product only. We relax the constraints on λ's and χ hypothetically in Case 1 and also the constraint on γ to an extent from the shock-tube CH_4 time history, all of which now vary from zero to two times of their respective nominal values. In that way, the constraint of χ can reach its upper physically possible bound. In Case 3, we examine the scenario when neither C_2H_4 nor CH_4 time history data is available, so that the α and β can take values over their respective physical ranges, while the ratio parameters are still loosely bound as in Case 2. Lastly, Case 4 extends the ratio parameters to ranges that correspond to random productions of C_2H_4, C_3H_6, 1-C_4H_8 and i-C_4H_8 with the mean ratio values equal to unity. The bound of γ is set to be its entire physical range. In this last case, a HyChem model is built largely from elemental balance only.

Using the MC approach, we generate random samples of reaction models using uniform distributions over the respective parameter ranges listed in Table 1. In all test cases, the rate coefficients k_{1-7} are also perturbed in terms of the pre-exponential A factor, within a factor of five from the respective nominal values, assuming a uniform distribution in log(k). For Cases 1 and 2 where C_2H_4 and/or CH_4 species data are imposed, we first generate the random model samples using the α, β, and γ bounds of Case 3, and then down-select the reaction models using the MC shooting method into a feasible set, all of which would predict the C_2H_4 and/or CH_4 time profiles within the respective bands as defined by the experimental uncertainty. Figure 1 shows the C_2H_4 profiles of a typical pyrolysis experiment taken from [23], which has been used for Jet A HyChem model development [2]. For all the C_2H_4 data considered in the earlier study of Jet A, the measurement uncertainty varies from 15 to 20%, depending on different test conditions [2,23]. We use the nominal simulated profile and calculate the 20% upper and lower bounds in the C_2H_4 profile, which is displayed as the shaded band in the figure. We choose the nominal model predictions to set up the uncertainty bounds and not the experimental data themselves because the nominal model prediction removes the random errors in each experiment, and it provides a more unbiased framework for sampling the experimental uncertainty. As illustrated in the figure, Model 1 (M1) is accepted

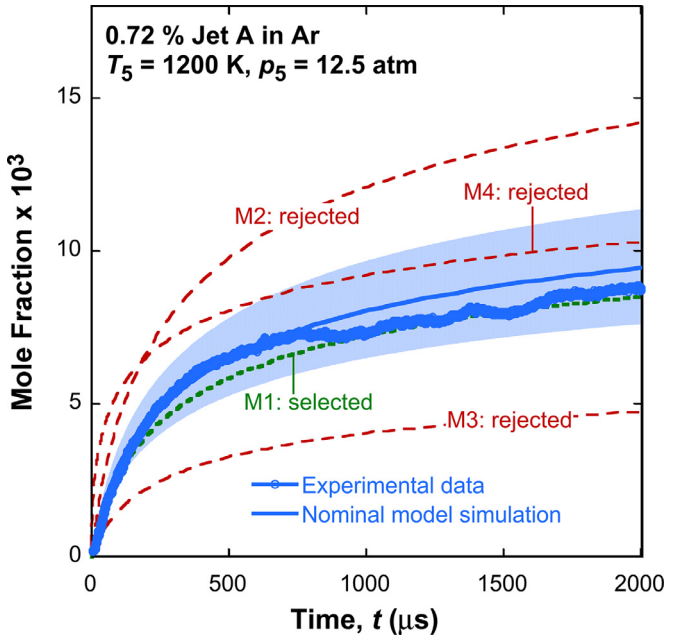

Fig. 1. Time histories of C_2H_4 from 0.72% (mole) Jet A under the conditions shown. Symbols: experimental data [23]; solid line: the nominal Jet A model simulation [2]; shaded band: the ±20% C_2H_4 uncertainty; dotted line: a MC model sample (M1) accepted into the feasible set; dashed lines (M2-M4): example model samples that are rejected.

Table 2
Thermodynamic conditions[a] of experiments for which Cases 1 & 2 model samples are derived.

No.	Reactant	p_5 (atm)	T_5 (K)
1	0.74% Jet A/Ar	12.4	1050
2	0.74% Jet A/Ar	12.4	1100
3	0.74% Jet A/Ar	12.4	1200
4	0.74% Jet A/Ar	12.4	1300
5	0.74% Jet A/Ar	12.4	1400
6	0.4% Jet A/6.6% O_2/Ar	1.6	1050
7	0.4% Jet A/6.6% O_2/Ar	1.6	1100
8	0.4% Jet A/6.6% O_2/Ar	1.6	1200

[a] The conditions were taken from shock tube experiments in [2].

into the feasible set, as its simulated C_2H_4 profile falls within the uncertainty bounds over the entire range of test time. Models 2–4 are rejected, each for a different reason. The above procedure is exercised for eight initial conditions, as listed in Table 2, spanning the ranges of the speciation data available over five pyrolysis and three oxidative pyrolysis cases. Ultimately, MC reaction models that satisfy all eight experimental conditions are adopted in the feasible set and used for subsequent τ_{ign} and S_u°evaluations.

4. Results and discussion

The results of all four MC cases are summarized in Fig. 2. Here, we use the ignition delay time (τ_{ign}) measured for Jet A-air mixtures at the equivalence ratio $\phi = 1.1$ and pressure behind reflect shock $p_5 = 10.9$ atm over a range of temperature, and the laminar flame speed of Jet A-air at an unburned temperature $T_u = 403$ K and pressure $p = 1$ atm over a range of equivalence ratio as our test cases. Both the experimental data of ignition delay time and laminar flame speed are taken from Ref. [2]. Several sets of ignition delay data are available; the set shown in Fig. 2 is chosen because it is the most representative data set of Jet A [2]. The probability distribution functions (PDFs) are obtained from 2000 MC model samples for each combustion property and each test case. Scatter plots of MC results are shown respectively in Figs. S1a-S1h of the Supplementary Material (SM).

Case 1 uses constraints from all measured species (C_2H_4, CH_4, C_3H_6, i-C_4H_8, 1-C_4H_8, C_6H_6, and C_7H_8). As it can be seen from Figs. 2a and 2b, the speciation data constrain the model well as far as predicting the global combustion properties is concerned: the τ_{ign} nominal prediction is in agreement with the experiment, and the τ_{ign} predicted uncertainty is approximately 50%, 60% and 90% at 1400, 1200 and 1000 K, respectively. We note that in the previous effort of HyChem model development, a limited number of ignition delay time data have been used to provide further guidance in parameter determination; while in Case 1, we impose no ignition delay constraints to the model. We will show in later text that with additional species considered, the τ_{ign} prediction uncertainty can be further reduced. Nevertheless, the uncertainty predicted for ignition delay in Case 1 is satisfactory above 1200 K, as the total uncertainty span is about factor of 2, which is comparable to the corresponding uncertainty in shock-tube ignition delay measurements. Suffice it to note that these uncertainty values are smaller than the model uncertainties resulting from the foundational fuel chemistry that lead to a uncertainty span size of τ_{ign} ranging from factor of 5 to an order of magnitude, as discussed in an earlier study [2].

The laminar flame speed is well predicted, and the speciation uncertainties have very little impact on the S_u°prediction, as the 2σ band is within ±1.5 cm/s. The predicted 2σ band is much lower than the experimental 2σ uncertainty, which varies from 2 to 5 cm/s. The results presented in Figs. 2a and 2b suggest that the HyChem-related experimental measurements are accurate enough for deriving the HyChem model parameters for predicting the ignition delay above 1200 K and laminar flame speed. Except for α, nearly all stoichiometric parameters are constrained well as seen by the corresponding PDFs in Figs. 3a-3g. In contrast, the rate coefficients are generally not constrained as well as the stoichiometric parameters, as shown in Figs. 3h-3n, in which the nominal rate parameters are shown for comparison. Four parameters (α, k_4, k_6, and k_7) are particularly under-constrained, because over the range of conditions considered, the thermal/oxidative pyrolysis rates are not sensitive to their values. Nonetheless, the nominal parameter values adopted in the HyChem model agree with the median values of the well-constrained parameters (i.e. γ, λ_3, $\lambda_{4,i}$, $\lambda_{4,1}$, χ, k_1, and k_3).

The increased ignition delay time prediction uncertainties for $T_5 < 1200$ K (Fig. 2a) can be explained by the sensitivity spectra with respect to the HyChem model parameters, as shown in Fig. 4. At 1400 K when fuel pyrolysis and the oxidation of the fuel fragments are fully decoupled, the τ_{ign} prediction is especially sensitive to λ_3 (i.e., the C_3H_6-to-C_2H_4 yield ratio). C_3H_6 is the second most dominant pyrolysis product from Jet A [2]. An increase in the λ_3 value decreases the reactivity of the pyrolyzed product mixture, and thus delays autoignition. Since the C_3H_6 uncertainty as measured in the flow reactor is quite small, the λ_3 value derived from it and the resulting ignition delay predictions are both quite accurate. In contrast, at the 1000 K initial temperature when the coupling of fuel thermal decomposition and the oxidation of the pyrolysis fragments is enhanced, λ_3 becomes a less important parameter since the production rates of the pyrolysis products (i.e. C_3H_6 and C_2H_4 here) are slow. At this temperature, β is now the dominant parameter because of its association with radical production from the fuel pyrolytic steps; and its impact amplifies toward lower temperatures. An increase in the β value enhances the production of H atom from fuel pyrolysis, thus enhancing both fuel decomposition and radical chain branching, leading to a shortened ignition delay.

To further illustrate the above point, we use two feasible Case 1 models (denoted as Models *a* and *b*) which predict nearly the same

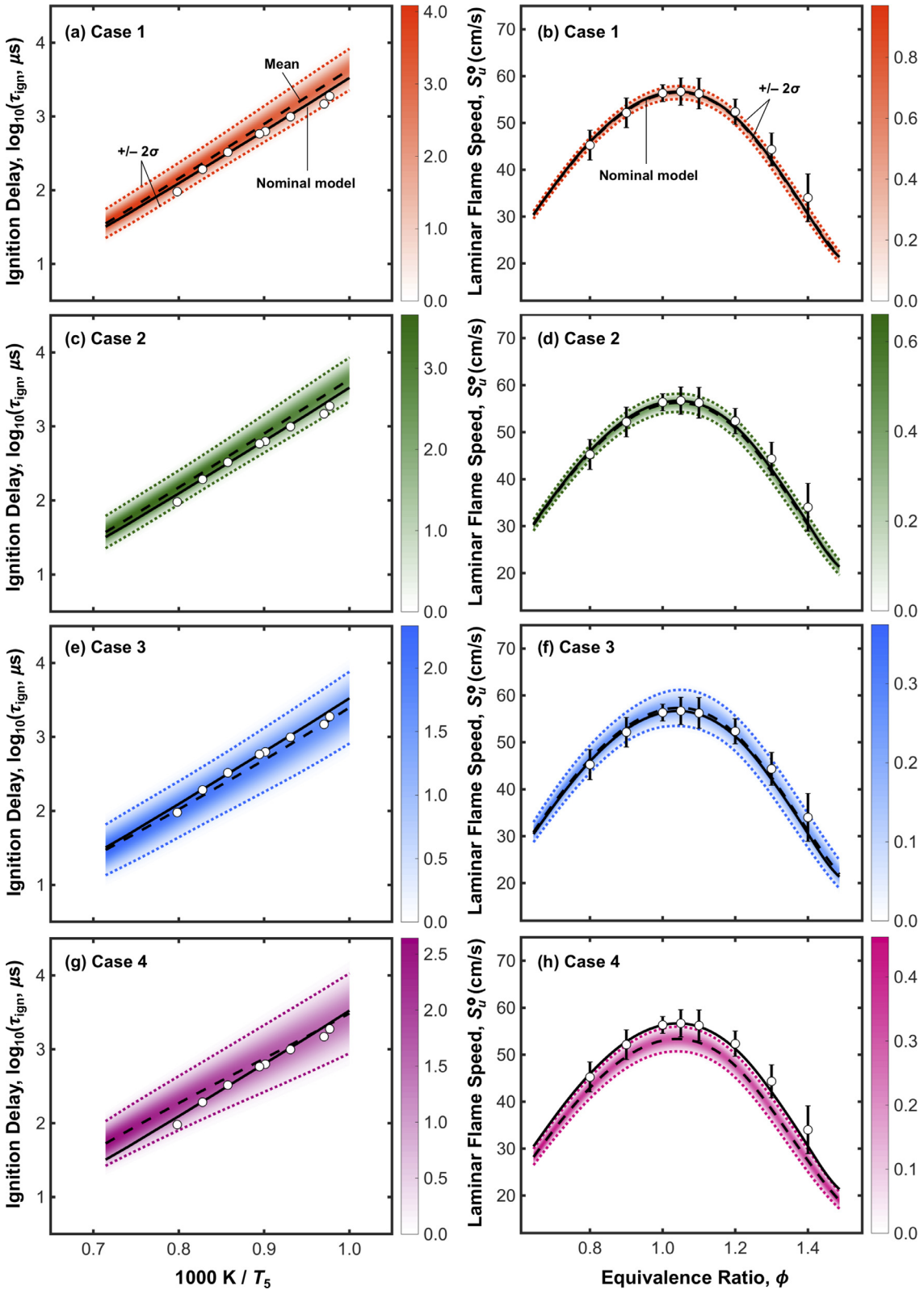

Fig. 2. Normalized probability distributions calculated for the ignition delay time (Jet A-air, $\phi = 1.1$, and $p_5 = 10.9$ atm) and laminar flame speed (Jet A-air, $T_u = 403$ K, and $p = 1$ atm), with intensities shown in the respective bars on the right side of the plots). Each distribution is derived from 2000 MC model samples for each of the four test cases. Open circles: experimental data taken from Ref. [2]; the error bars on the flame speed data are the 2σ uncertainties; solid lines: predictions of the nominal Jet A model [2]; dashed lines: means of the model predictions; dotted lines: 2σ bounds of the model predictions. (For interpretation of the references to colour in this figure legend, the reader is referred to the web version of this article.)

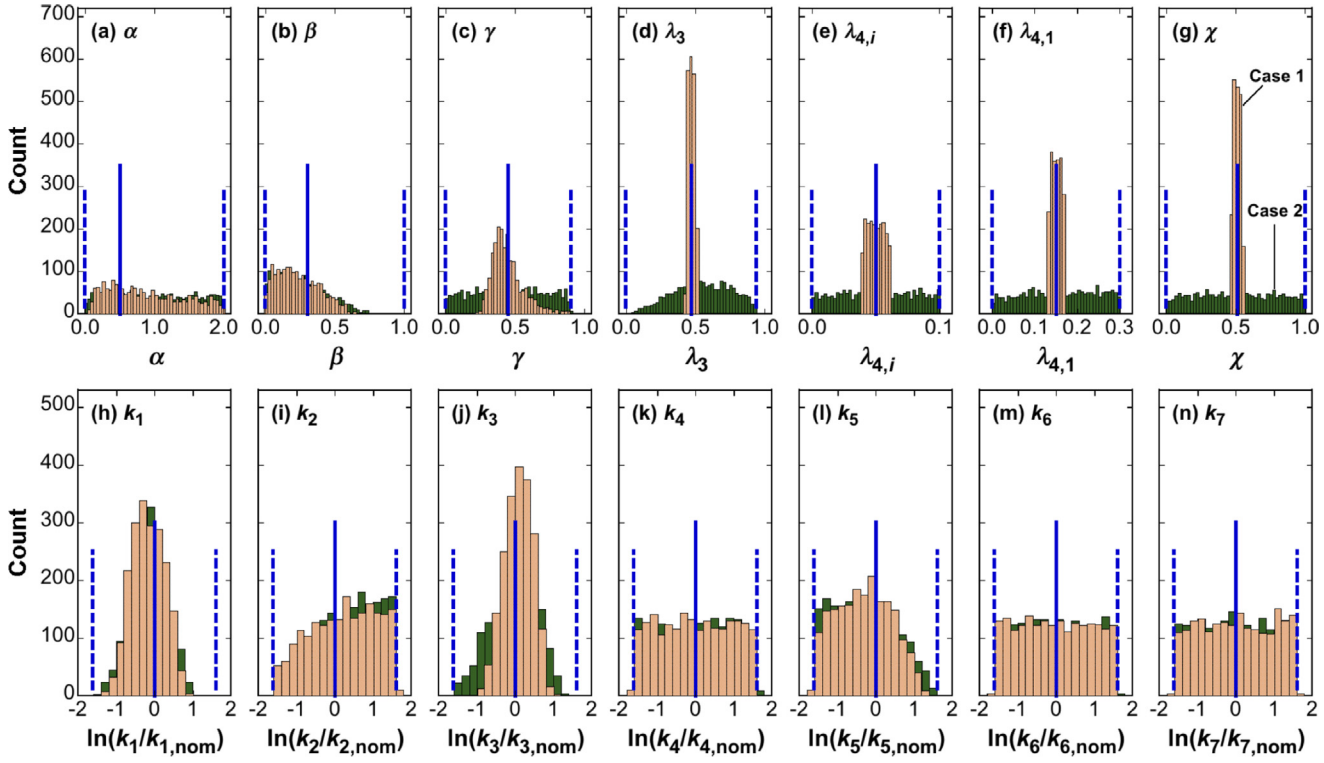

Fig. 3. Probability distributions of seven stoichiometric parameters compared to their respective nominal values (a-g, top panel) and seven rate coefficients normalized by their respective nominal values (h-n, bottom panel), computed for Cases 1 and 2. Solid line: nominal values in the Jet A HyChem model; dashed line: the initial parameter bounds from Case 3. (For interpretation of the references to colour in this figure legend, the reader is referred to the web version of this article.)

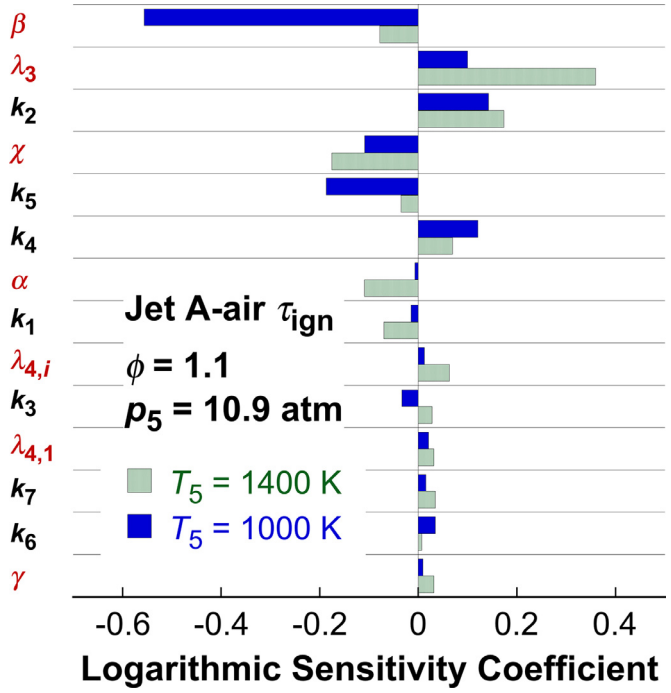

Fig. 4. Logarithmic sensitivity coefficients of ignition delay time computed for Jet A-air mixture under the conditions shown with respect to HyChem model parameters.

ignition delay time at 1400 K, but have significantly different values at 1000 K. The values of the 14 independent parameters of the two models are listed in Table S1 of the Supplementary Material. As shown, the λ_3 value differs by only 10% between the two model parameter sets, while the β value in Model *b* is a factor of 3 of that in Model *a*. The differences among other parameters vary to different extents. Nevertheless, Fig. 5 shows the key species profiles at the 1400 and 1000 K initial temperature. Clearly, at 1400 K, fuel pyrolysis and the oxidation of pyrolysis products (e.g. C_2H_4 shown here) are decoupled in time, and the two models predict almost identical temporal structures leading to ignition. At 1000 K, however, both models show increased coupling between fuel decomposition and oxidation of fuel fragments. This extended coupling is primarily due to the lower rates of fuel pyrolysis. Moreover, at 1000 K, Model *b* predicts the early-stage H radical concentration to be five times that of Model *a*. This difference leads to quite substantial difference in the fuel pyrolytic rates. Although the peak C_2H_4 yields are almost identical, Model *b* still predicts a nearly 50% shorter τ_{ign} than Model *a*. Besides of the difference in the H concentration, CH_2O and CO, which are commonly identified as key species involved in first-stage ignition processes, also exhibit different production rates. At around 1000 K, their production and destruction rates become closely coupled to the fuel decomposition chemistry, again because of the increased coupling between fuel pyrolysis and the oxidation of the pyrolysis products.

The sensitivities shown for CO and CH_2O suggest that these species could be critical to remedying the inability of the current HyChem model to more accurately predict ignition delay toward its lower temperature bound of applicability. Figure 6 presents the sensitivity spectra of several key species with respect to the 14 HyChem parameters computed for a 0.4% Jet A/6.6% O_2/Ar mixture at 1050 K initial temperature and 1.6 atm constant pressure. The spectra are calculated using the species concentrations (x) at 2 ms reaction time under Condition 6 of Table 2 (T_5 = 1050 K). The sensitivity coefficient is defined as $S = [\Delta x]_{2\times p} / [\Delta x]_p - 1$, where $\Delta x = x(t = 2\text{ ms}) - x(t = 0)$ and p refers to any of the 14 model parameters. It is seen that under the condition shown, CO production is sensitive to the parameters that govern radical pool buildup, including α, β, k_2 ($C_mH_n + H$), and k_4 (C_mH_n + OH).

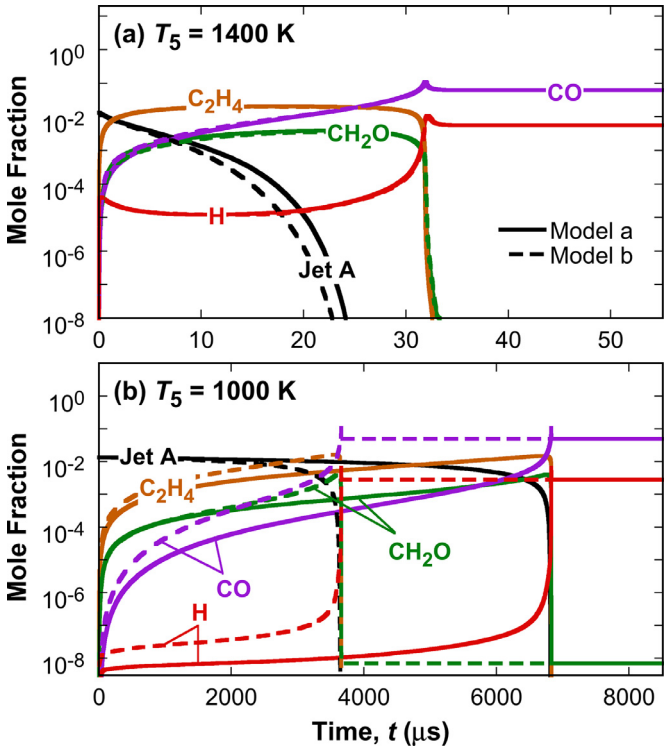

Fig. 5. Time histories of mole fractions computed for key species using sample Models *a* (solid lines) and *b* (dashed lines) for Jet A-air ignition at 1400 K (a) and 1000 K (b) initial temperature, 1.1 equivalence ratio and 10.9 atm initial pressure.

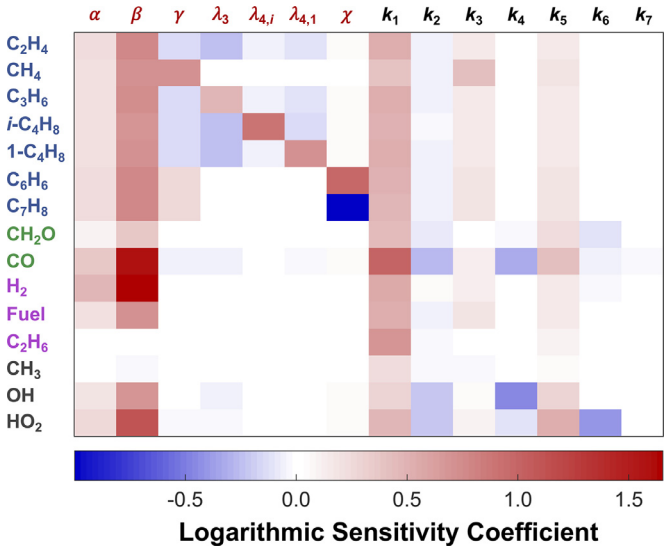

Fig. 6. Logarithmic sensitivity spectra of selected species with respect to HyChem parameters computed for 0.4% Jet A/6.6% O_2/Ar reaction at 1050 K initial temperature and 1.6 atm constant pressure. The sensitivity coefficient is defined as $S = [\Delta x]_{2\times p} / [\Delta x]_p - 1$, where $\Delta x = x(t = 2\ \text{ms}) - x(t = 0)$ and p refers to any of the 14 HyChem parameters.

The sensitivity spectra of CH_2O are similar to CO, but with weaker intensities. Nevertheless, the results shown here suggest that CO and CH_2O are the additional measurement targets to reduce the HyChem model uncertainty in the 1000 K to 1200 K temperature range, especially considering that laser diagnostics of CO [24,25] and CH_2O [26,27] are well-developed for shock tubes. Additionally, CO and CH_2O can be measured in other legacy experimental facilities such as jet stirred reactors and flow reactors (see, for example, [4,17,28-32]). Furthermore, the CO speciation is helpful to reducing τ_{ign} prediction uncertainties above 1200 K also, because of its strong sensitivity to k_2, k_4 and β. In particular, the results of Fig. 4 suggest that k_2 is important for the ignition delay time prediction at the 1400 K initial temperature, as Reaction (R2) contributes to H-radical removal, and this can impact both the pyrolysis and oxidation processes. Since k_2 is loosely constrained by the current set of speciation data (see Fig. 3i), introducing CO as a target species would benefit HyChem model accuracy.

Additionally, hydrogen (H_2) production and fuel consumption exhibit very strong sensitivity to β and their measurement would impose a strong constraint on this parameter. While H_2 can be measured using combined gas chromatography and mass spectrometry technique (GC–MS) [30], fuel consumption is more challenging because of its multicomponent nature. In an earlier phase of HyChem model development, one set of H_2 and fuel (Jet A) data from flow reactor experiment were consulted [2], and these data were indeed found to be useful. Other species that can be utilized in HyChem model development include C_2H_6 by GC–MS [30], and CH_3, OH, and HO_2, all of which are amenable to laser diagnostics [33-35].

We assess the impact of C_2H_4 speciation next (Case 2 of Table 1). Figure 2c and d show the PDFs of model predictions of Case 2. As it can be seen, C_2H_4 speciation alone is sufficient for deriving the HyChem model parameters at least for the conditions tested. The nominal predictions for the ignition delay (τ_{ign}) and laminar flame speed (S_u°) are in close agreement with the experimental data. This is not surprising considering that $C_2H_4$is the most dominant product from Jet A pyrolysis, accounting for up to 1/3 of total carbon yield [1,2,23,36]. The PDFs of the 14 independent parameters shown in Fig. 3 suggest that β, k_1, and k_3 are primarily constrained by the C_2H_4 speciation data, and other parameters, e.g., λ_3, k_2, and k_5, are constrained by the same data to an extent. Importantly, the current analysis illustrates yet another example concerning the importance of ethylene diagnostics in the high-temperature combustion chemistry of hydrocarbons. Without experimental constrains beyond C_2H_4, the 2σ prediction spans expectedly increase as compared to those of Case 1. The 2σ values in $S_u^\circ$are now ± 2 cm/s, and the uncertainties in τ_{ign} are $< 70\%$ above 1200 K, leading to a total span size of τ_{ign} to be within factor of 3 of the nominal prediction and the experimental data.

If we take away the constraint of C_2H_4 along with all other speciation data, a HyChem model would be developed essentially from elemental conservations. Cases 3 and 4 are such cases, varying the degree of the constraints on the stoichiometric parameters that range from an educated guess (Case 3) to practically unconstrained case except for the expectation of equal, statistical importance of C_2H_4, C_3H_6, i-C_4H_8, and 1-C_4H_8 as the Jet A pyrolysis products (Case 4). In both cases, α, β, and χ span their respective physical ranges. In Case 3, the bounds of λ's, and γ remain the same as those for Case 2. In Case 4, the upper bounds of λ's are relaxed to 2, so the mean values of these ratio parameters are unity. Overall, Case 4 allows the model prediction to be less impacted by C_2H_4 and more influenced by C_3 and C_4 alkene species, which generally lead to reduced high-temperature oxidation rate, because the oxidation of i-C_4H_8 and C_3H_6 is notably slower than that of C_2H_4 [3].

To understand the last two cases tested, we first plot in Fig. 7 the PDFs of the yields of C_2H_4, i-C_4H_8, and C_3H_6 from Jet A pyrolysis. Each yield value is calculated from a set of stoichiometric parameters sampled; 2000 such MC samples are generated for each case. Here, we assume that all pyrolysis products are produced from H-abstraction reactions (R2–R7) without coupling with

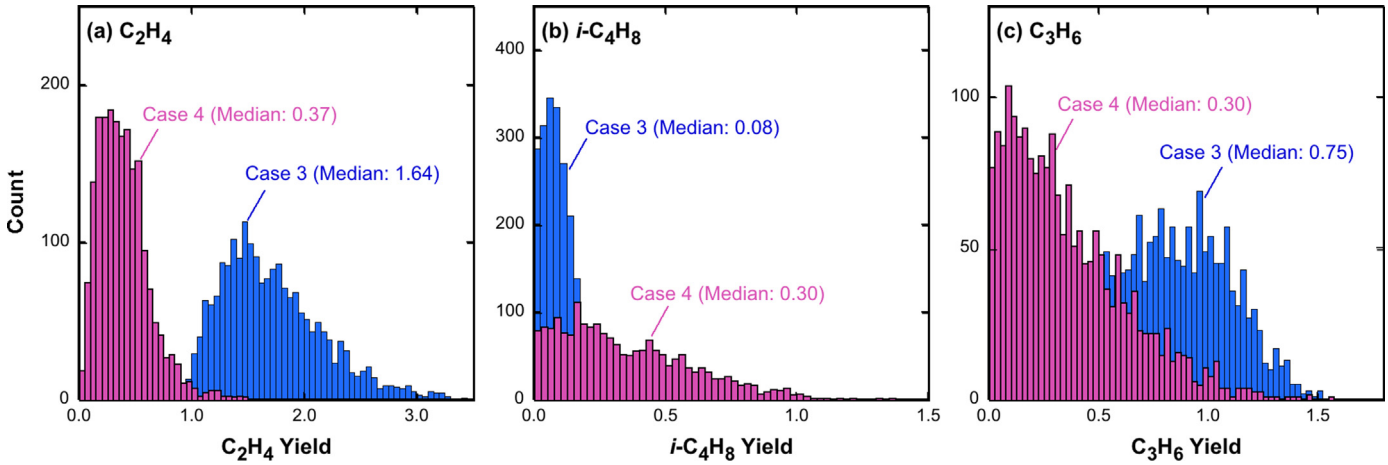

Fig. 7. C_2H_4 (a), i-C_4H_8 (b), and C_3H_6 (c) yields calculated from Eqns. (5), (6), and (7) using the stoichiometric parameters in 2000 MC samples for each test cases.

secondary reactions. Therefore, from Eqn. (2), the yields of C_2H_4, i-C_4H_8, and C_3H_6 may be derived from elemental balance as:

$$y_{C_2H_4,\text{elementalbalance}} \cong e_a = \frac{[-(4-\chi)m + (7-\chi)n/2 + 3\beta - (10-\chi)\gamma - (10-\chi)]}{3(2+3\lambda_3+4\lambda_{4,i}+4\lambda_{4,1})} \tag{5}$$

$$y_{i\text{-}C_4H_8,\text{elementalbalance}} \cong e_a\lambda_{4,i} = \frac{[-(4-\chi)m + (7-\chi)n/2 + 3\beta - (10-\chi)\gamma - (10-\chi)]}{3(2+3\lambda_3+4\lambda_{4,i}+4\lambda_{4,1})}\lambda_{4,i} \tag{6}$$

$$y_{C_3H_6,\text{elementalbalance}} \cong e_a\lambda_3 = \frac{[-(4-\chi)m + (7-\chi)n/2 + 3\beta - (10-\chi)\gamma - (10-\chi)]}{3(2+3\lambda_3+4\lambda_{4,i}+4\lambda_{4,1})}\lambda_3 \tag{7}$$

As shown in Fig. 7, the dominance of C_2H_4 as a pyrolysis product becomes weaker from Case 3 to Case 4 as the median C_2H_4 yield decreases by about factor of 5, from 1.64 to 0.37. On the other hand, the median yield of i-C_4H_8 increases from 0.08 in Case 3 to 0.30 in Case 4. Additionally, the median C_3H_6 yield decreases from 0.75 in Case 3 to 0.30 in Case 4.

The results computed for the ignition delay and laminar flame speed are shown in Fig. 2e through 2h. Informed essentially by elemental conservations, Case 3 shows that the mean values of τ_{ign} and $S_u^\circ$are still in close agreement with the experimental data, while the mean values in Case 4 deviate from the experiments, even though model predictions span surprisingly small ranges in both cases. For Case 3, the uncertainty span size in τ_{ign} is within an order of magnitude ($\times$ /÷3 the mean value), and the mean value of the probability distribution is within 25% of the experimental data and nominal model predictions. For S_u°, the predictions lie in $a \pm 4$ cm/s 2σ band, which is comparable to the 2σ experimental uncertainty. In Case 4, the mean value of the probability distribution of τ_{ign} starts to deviate from the nominal model prediction above 1250 K, and the mean value of the S_u°distributions are lower than the value predicted by nomial Jet A model. Clearly, the slower oxidation behavior predicted is associated with decreased productions of C_2H_4, and increases in the less reactive intermediates (e.g. i-C_4H_8) as discused earlier.

To illustrate the above point, we plot in Fig. 8a and b the simulated S_u°values at 1.04 equivalence ratio as functions of C_2H_4 and i-C_4H_8 yields using 500 MC samples combined under Cases 3 and 4. Again, the C_2H_4 and i-C_4H_8 yields are calculated from Eqs. (5) and (6), respectively. Clearly, from Case 3 to 4, the dependency of laminar flame speed prediction on C_2H_4 becomes much weaker, while such dependency turns stronger on i-C_4H_8. Similarly, Fig. 8c and d present the same set of simulated S_u°values as functions of C_2H_4 and C_3H_6 yields under Cases 3 and 4. In Case 3, when C_2H_4 and C_3H_6 are the top two most dominant pyrolysis products, the laminar flame speed shows stronger dependencies on C_2H_4 than C_3H_6. However, in Case 4 when both species yields are reduced and being equal, laminar flame speed is still more sensitive to C_2H_4 than C_3H_6. Overall, the tests shown in Fig. 8 illustrate that (a) the laminar flame speed is the most sensitive to the C_2H_4 yield from the fuel – an increase in the C_2H_4 yield causes the flame speed to increase, and (b) an increase in the i-C_4H_8 or C_3H_6 yield reduces the flame speed, and the effect of i-C_4H_8 appears to be larger. Analyses of the reaction fluxes and sensitivities indicate that the attack of i-C_4H_8 and C_3H_6 by the H-atom both lead to effective H-atom recombination, i.e.,

$$i\text{-}C_4H_8 + H \rightarrow i\text{-}C_4H_7 + H_2$$

$$i\text{-}C_4H_7 + H\ (+M) \rightarrow i\text{-}C_4H_8\ (+M)$$

$$C_3H_6 + H \rightarrow a\text{-}C_3H_5 + H_2$$

$$a\text{-}C_3H_5 + H\ (+M) \rightarrow C_3H_6\ (+M)$$

where i-C_4H_7 is the methylpropenyl radical ($H_2C{=}C(CH_3)C{\bullet}H_2$) and a-C_3H_5 is the allyl radical ($H_2C{=}C(H)C{\bullet}H_2$), both of which are resonantly stabilized and resistant against further decomposition or oxidation. In contrast, the H-abstraction of C_2H_4 produces the vinyl radical (C_2H_3), which decomposes readily to C_2H_2 + H or reacts with O_2 to form CH_2O + HCO and CH_2CHO + O, all of which speed up the radical buld-up.

The effect of the rate coefficients on the prediction of ignition delay time and laminar flame speed is significantly smaller than the stoichiometric parameters, as stated before. Results of sensitivity analyses with 10 $\times$ and 2 $\times$ the rate coefficient perturbation are provided in Fig. S2 as probability distributions and in Fig. S3 as scatter plots, and these are compared to the results obtained with 5 $\times$ the rate coefficient perturbation, all for Case 3. As shown in Figs. S2b and S2d, the S_u°prediction is insensitive to the rate coefficient perturbation. Such insensitivity is expected, since $S_u^\circ$is mostly sensitive to foundational fuel chemistry (e.g. H + O_2 = OH + O and CO + OH = CO_2 + H) [2]. As for the τ_{ign} prediction, the size of the prediction uncertainty band increases from 2 $\times$ to 10 $\times$ rate perturbations, which are primarily caused by k_2, k_4, and k_5. However, we note that the impact of the rate coefficients ($k_{1\text{-}7}$) is generally smaller than that of the stoichiometric parameters especially for T > 1200 K (see, Fig. 4). Under this condition, the oxidative pyrolysis

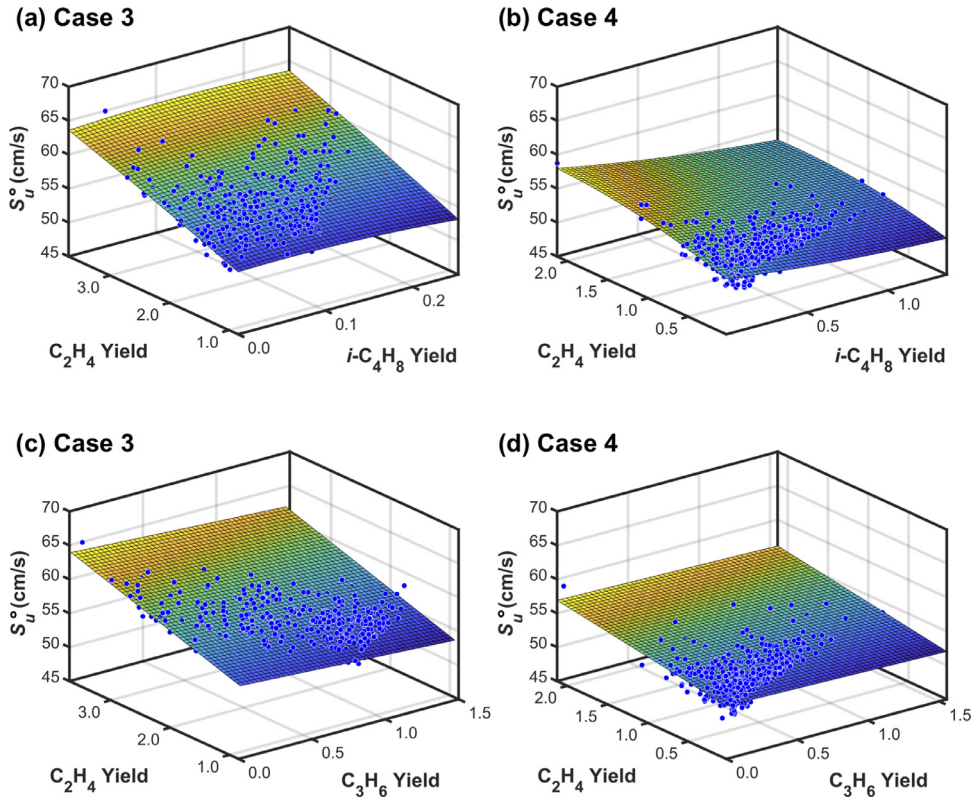

Fig. 8. Simulated laminar flame speed of the Jet A-air mixture at 403 K unburned temperature, 1 atm pressure, and 1.04 equivalence ratio as functions of C_2H_4 and i-C_4H_8 yields (top panels), and as functions of C_2H_4 and C_3H_6 yields (bottom panels), using 500 MC reaction models under (a) & (c) Case 3, (b) & (d) Case 4. The C_2H_4, i-C_4H_8, and C_3H_6 yields are calculated from elemental balance Eqs. (5), (6), and (7), respectively. The 2D surface shown in each figure is a 2nd order polynomial fit to guide the eyes.

time is much shorter than the time for the oxidation of the pyrolysis products, and as such, the choices of the rate coefficients are not particularly important.

Lastly, another interesting message that we can extract also from the results of Case 4 is that when no experimental speciation information is available, a HyChem model formulated essentially by elemental conservation can be reasonably predictive as far as ignition delay time and laminar flame speed are concerned. Because all of the modern reaction models along with the relevant computer codes explicitly or implicity impose elemental conservation, any such model is expected to predict the global combustion properties of real, liquid fuels well as long as its foundational fuel chemistry submodel is reaonably accurate.

5. Conclusions

The predictive capability of the HyChem model is evaluated in the context of experimental speciation data in shock tube and flow reactor using the Jet A fuel and its HyChem reaction model as the test case. We assessed the impact of C_2H_4, CH_4, C_3H_6, i-C_4H_8, 1-C_4H_8, C_6H_6 and C_7H_8 speciation measurements on the ability of the HyChem model to predict ignition delay time and laminar flame speed. The following conclusions are reached:

(1) With the available speciation data, the HyChem Jet A model is mathematically closed with respect to its predictions of the laminar flame speed and of shock tube ignition delay time above 1200 K initial temperature, even though some of the model parameters remain under-constrained or even unconstrained.

(2) The uncertainties for the predicted ignition delay remain disturbingly large below 1200 K. To this end, CO and CH_2O speciation from oxidative pyrolysis of the fuel hold the potential for drastically improving the HyChem predictive confidence under that condition. CO and CH_2O can be measured in a shock tube using well-developed laser diagnostic techniques, and they can also be accessed by other experimental facilities, such as jet stirred reactors and flow reactors.

(3) In absence of any meaningful experimental information about the fuel pyrolysis products, the HyChem formulation derived on elemental conservation only can predict ignition delay time of fuel-air mixtures to a reasonable degree of accuracy: under the worst case scenario, within an order of magnitude ($\times$ /$\div$ 3 the mean value) for ignition delay times above the 1000 K initial temperature and within $\pm$4 cm/s for laminar flame speed at atmospheric pressure across a fairly wide range of equivalence ratio.

Finally, we note that reliable laser diagnostics of ethylene and other related species, developed in Professor Ronald Hanson's laboratory over the past two decades, prove to be critical to HyChem model development in two related aspects. First, the diagnostic capability provides the intellectual underpinning for the HyChem approach, in that it enables a cause-and-effect argument underlying the HyChem approach. Second, the reliable laser diagnostic technique is crucial to developing a predictive HyChem model for any real, liquid fuels with limited number of experiments without even knowing its detailed composition.

Declaration of Competing Interest

The authors declare that they have no known competing financial interests or personal relationships that could have appeared to influence the work reported in this paper.

Acknowledgement

The work was supported by the Air Force Office of Scientific Research under grant number FA9550-16-1-0195 under the technical monitoring of Dr. Chiping Li. The authors wish to thank their collaborators on the HyChem project, including Professors F. N. Egolfopoulos, K. Brezinsky, T.-F. Lu, C. T. Bowman, and especially R. K. Hanson for their effort and support.

Supplementary materials

Supplementary material associated with this article can be found, in the online version, at doi:10.1016/j.combustflame.2020.10.023.

References

[1] H. Wang, R. Xu, K. Wang, C.T. Bowman, R.K. Hanson, D.F. Davidson, K. Brezinsky, F.N. Egolfopoulos, A physics-based approach to modeling real-fuel combustion chemistry – I. Evidence from experiments, and thermodynamic, chemical kinetic and statistical considerations, Combust. Flame 193 (2018) 502–519.

[2] R. Xu, K. Wang, S. Banerjee, J. Shao, T. Parise, Y. Zhu, S. Wang, A. Movaghar, D.J. Lee, R. Zhao, X. Han, Y. Gao, T. Lu, K. Brezinsky, F.N. Egolfopoulos, D.F. Davidson, R.K. Hanson, C.T. Bowman, H. Wang, A physics-based approach to modeling real-fuel combustion chemistry – II. Reaction kinetic models of jet and rocket fuels, Combust. Flame 193 (2018) 520–537.

[3] K. Wang, R. Xu, T. Parise, J. Shao, A. Movaghar, D.J. Lee, J.-.W. Park, Y. Gao, T. Lu, F.N. Egolfopoulos, D.F. Davidson, R.K. Hanson, C.T. Bowman, H. Wang, A physics-based approach to modeling real-fuel combustion chemistry – IV. HyChem modeling of combustion kinetics of a bio-derived jet fuel and its blends with a conventional Jet A, Combust. Flame 198 (2018) 477–489.

[4] Y. Tao, R. Xu, K. Wang, J. Shao, S.E. Johnson, A. Movaghar, X. Han, J.-.W. Park, T. Lu, K. Brezinsky, F.N. Egolfopoulos, D.F. Davidson, R.K. Hanson, C.T. Bowman, H. Wang, A Physics-based approach to modeling real-fuel combustion chemistry – III. Reaction kinetic model of JP10, Combust. Flame 198 (2018) 466–476.

[5] R. Xu, C. Saggese, R. Lawson, A. Movaghar, T.C. Parise, J. Shao, R. Choudhary, J.-.W. Park, T. Lu, R.K. Hanson, D.F. Davidson, F.N. Egolfopoulos, A. Aradi, A. Prakash, V.R.R. Mohan, R. Cracknell, H. Wang, A physics-based approach to modeling real-fuel combustion chemistry – VI. Reaction kinetic models of gasoline fuels, Combust. Flame 220 (2020) 475–487.

[6] X. Zhao, Y. Tao, T. Lu, H. Wang, Sensitivities of direct numerical simulations to chemical kinetic uncertainties: spherical flame kernel evolution of a real jet fuel, Combust. Flame 209 (2019) 117–132.

[7] C. Xu, A.Y. Poludnenko, X. Zhao, H. Wang, T. Lu, Structure of strongly turbulent premixed *n*-dodecane–air flames: direct numerical simulations and chemical explosive mode analysis, Combust. Flame 209 (2019) 27–40.

[8] L. Esclapez, P.C. Ma, E. Mayhew, R. Xu, S. Stouffer, T. Lee, H. Wang, M. Ihme, Fuel effects on lean blow-out in a realistic gas turbine combustor, Combust. Flame 181 (2017) 82–99.

[9] A. Felden, L. Esclapez, E. Riber, B. Cuenot, H. Wang, Including real fuel chemistry in LES of turbulent spray combustion, Combust. Flame 193 (2018) 397–416.

[10] P. Glarborg, J.A. Miller, B. Ruscic, S.J. Klippenstein, Modeling nitrogen chemistry in combustion, Prog. Energy Combust. Sci. 67 (2018) 31–68.

[11] C. Saggese, K. Wan, R. Xu, Y. Tao, C.T. Bowman, J.-.W. Park, T. Lu, H. Wang, A physics-based approach to modeling real-fuel combustion chemistry – V. NO_x formation from a typical Jet A, Combust. Flame 212 (2020) 270–278.

[12] K. Wang, C.T. Bowman, H. Wang, Kinetic analysis of distinct product generation in oxidative pyrolysis of four octane isomers, Proc. Combust. Inst. 37 (2019) 531–538.

[13] E. Ranzi, M. Dente, A. Goldaniga, G. Bozzano, T. Faravelli, Lumping procedures in detailed kinetic modeling of gasification, pyrolysis, partial oxidation and combustion of hydrocarbon mixtures, Prog. Energy Combust. Sci. 27 (2001) 99–139.

[14] S. Li, B. Varatharajan, F. Williams, Chemistry of JP-10 ignition, AIAA J. 39 (2001) 2351–2356.

[15] B. Varatharajan, M. Petrova, F. Williams, V. Tangirala, Two-step chemical-kinetic descriptions for hydrocarbon–oxygen-diluent ignition and detonation applications, Proc. Combust. Inst. 30 (2005) 1869–1877.

[16] M. Colket, T. Edwards, S. Williams, N.P. Cernansky, D.L. Miller, F. Egolfopoulos, P. Lindstedt, K. Seshadri, F.L. Dryer, C.K. Law, D. Friend, D.B. Lenhert, H. Pitsch, A. Sarofim, M. Smooke, W. Tsang, Development of an experimental database and kinetic models for surrogate jet fuels, 45th AIAA Aerospace Sciences Meeting and Exhibit, Reno, NV, USA, 2007.

[17] S. Dooley, S.H. Won, M. Chaos, J. Heyne, Y. Ju, F.L. Dryer, K. Kumar, C.-J. Sung, H. Wang, M.A. Oehlschlaeger, R.J. Santoro, T.A. Litzinger, A jet fuel surrogate formulated by real fuel properties, Combust. Flame 157 (2010) 2333–2339.

[18] M. Colket, J. Heyne, M. Rumizen, M. Gupta, T. Edwards, W.M. Roquemore, G. Andac, R. Boehm, J. Lovett, R. Williams, J. Condevaux, D. Turner, N. Rizk, J. Tishkoff, C. Li, J. Moder, D. Friend, V. Sankaran, Overview of the national jet fuels combustion program, AIAA J. 55 (2017) 1087–1104.

[19] H. Wang, X. You, A.V. Joshi, S.G. Davis, A. Laskin, F. Egolfopoulos, C.K. Law, USC Mech Version II. High-temperature combustion reaction model of H2/CO/C1-C4 compounds. http://ignis.usc.edu/Mechanisms/USC-Mech%20II/USC_Mech%20II.htm, 2007.

[20] H. Wang, E. Dames, B. Sirjean, D.A. Sheen, R. Tangko, A. Violi, J.Y.W. Lai, F.N. Egolfopoulos, D.F. Davidson, R.K. Hanson, C.T. Bowman, C.K. Law, W. Tsang, N.P. Cernansky, D. Millar, R.P. Lindstedt, A high-temperature chemical kinetic model of *n*-alkane (up to *n*-dodecane), cyclohexane, and methyl-, ethyl-, *n*-propyl and *n*-butyl-cyclohexane oxidation at high temperatures, JetSurF version 2.0, September 19, 2010 (http://web.stanford.edu/group/haiwanglab/JetSurF/JetSurF2.0/index.html).

[21] R.J. Kee, F.M. Rupley, J.A. Miller, Chemkin-II: a Fortran chemical kinetics package for the analysis of gas-phase chemical kinetics, Report No. SAND-89-8009, Sandia National Laboratories, 1989.

[22] R.J. Kee, J.F. Grcar, M.D. Smooke, J. Miller, E. Meeks, PREMIX: a Fortran program for modeling steady laminar one-dimensional premixed flames, Report No. SAND85-8249, Sandia National Laboratories, 1985.

[23] J. Shao, Y. Zhu, S. Wang, D.F. Davidson, R.K. Hanson, A shock tube study of jet fuel pyrolysis and ignition at elevated pressures and temperatures, Fuel 226 (2018) 338–344.

[24] W. Ren, E. Dames, D. Hyland, D.F. Davidson, R.K. Hanson, Shock tube study of methanol, methyl formate pyrolysis: CH_3OH and CO time-history measurements, Combust. Flame 160 (2013) 2669–2679.

[25] S. Wang, D.F. Davidson, R.K. Hanson, Shock tube and laser absorption study of CH_2O oxidation via simultaneous measurements of OH and CO, J. Phys. Chem. A 121 (2017) 8561–8568.

[26] G. Friedrichs, D.F. Davidson, R.K. Hanson, Direct measurements of the reaction H + CH_2O → H_2 + HCO behind shock waves by means of Vis–UV detection of formaldehyde, Int. J. Chem. Kinet. 34 (2002) 374–386.

[27] S. Wang, D.F. Davidson, R.K. Hanson, High-temperature laser absorption diagnostics for CH_2O and CH_3CHO and their application to shock tube kinetic studies, Combust. Flame 160 (2013) 1930–1938.

[28] T. Held, F. Dryer, An experimental and computational study of methanol oxidation in the intermediate-and high-temperature regimes, Symp. (Int.) Combust. 25 (1994) 901–908.

[29] S. Dooley, S.H. Won, J. Heyne, T.I. Farouk, Y. Ju, F.L. Dryer, K. Kumar, X. Hui, C.-J. Sung, H. Wang, The experimental evaluation of a methodology for surrogate fuel formulation to emulate gas phase combustion kinetic phenomena, Combust. Flame 159 (2012) 1444–1466.

[30] S. Banerjee, R. Tangko, D.A. Sheen, H. Wang, C.T. Bowman, An experimental and kinetic modeling study of *n*-dodecane pyrolysis and oxidation, Combust. Flame 163 (2016) 12–30.

[31] A. Mzé-Ahmed, K. Hadj-Ali, P. Diévart, P. Dagaut, Kinetics of oxidation of a synthetic jet fuel in a jet-stirred reactor: experimental and modeling study, Energy Fuels 24 (2010) 4904–4911.

[32] P. Dagaut, F. Karsenty, G. Dayma, P. Diévart, K. Hadj-Ali, A. Mzé-Ahmed, M. Braun-Unkhoff, J. Herzler, T. Kathrotia, T. Kick, Experimental and detailed kinetic model for the oxidation of a Gas to Liquid (GtL) jet fuel, Combust. Flame 161 (2014) 835–847.

[33] M.A. Oehlschlaeger, D.F. Davidson, R.K. Hanson, High-temperature UV absorption of methyl radicals behind shock waves, J. Quant. Spectrosc. Ra. 92 (2005) 393–402.

[34] S.S. Vasu, D.F. Davidson, Z. Hong, V. Vasudevan, R.K. Hanson, *n*-Dodecane oxidation at high-pressures: measurements of ignition delay times and OH concentration time-histories, Proc. Combust. Inst. 32 (2009) 173–180.

[35] Z. Hong, K.-.Y. Lam, R. Sur, S. Wang, D.F. Davidson, R.K. Hanson, On the rate constants of OH + HO_2 and HO_2 + HO_2: a comprehensive study of H_2O_2 thermal decomposition using multi-species laser absorption, Proc. Combust. Inst. 34 (2013) 565–571.

[36] X. Han, M. Liszka, R. Xu, K. Brezinsky, H. Wang, A high pressure shock tube study of pyrolysis of real jet fuel Jet A, Proc. Combust. Inst. 37 (2019) 189–196.